Chapter 3

Electrodynamics of Evanescent Wave in Negative Refractive Index Superlens

Wei Li and Xunya Jiang

Additional information is available at the end of the chapter

http://dx.doi.org/10.5772/50025

1. Introduction

Early in 1968, Veselago[1] predicted that a new type of artificial metamaterial, which possesses simultaneously negative permittivity and permeability, could function as a lens to focus electromagnetic waves. These research direction was promoted by Pendry's work[2, 3] and other latter works [4–26]. They show that with such a metamaterial lens, not only the radiative waves but also the evanescent waves, can be collected at its image, so the lens could be a superlens which can break through or overcome the diffraction limit of the conventional imaging system. This beyond-limit property gives us a new window to design devices.

It is well-known that evanescent wave plays an important role in the beyond-limit property of the metamaterial superlens. Furthermore, evanescent waves become more and more important when the metamaterial devices enter sub-wavelength scales[27, 28]. Therefore, the quantitatively study of *pure* evanescent waves in the metamaterial superlens is very significant. However, the quantitatively effects of *pure* evanescent wave in the metamaterial superlens have not been intensively studied, since so far almost all studies were only interested in the image properties with global field[8, 9], which is the summation of radiative wave and evanescent wave. On the other hand, many theoretical works were performed to study the metamaterial superlens, employing either finite-difference-time domain (FDTD) simulations[16] or some approximate approaches[29, 30]. However, one cannot obtain the rigorous *pure* evanescent wave by these numerical methods, since the image field of the metamaterial superlens obtained by FDTD is global field, and other approximate approaches cannot be rigorous.

In reviewing these existing efforts, we feel desirable to develop a rigorous method that can be used to study quantitatively the transient phenomena of the evanescent wave in the image of the metamaterial superlens. In this paper, we will present a new method based on the Green's function[7, 8] to serve this purpose. Our method can be successfully used to calculate the evanescent wave, as well as the radiative wave and the global field. The main idea of our method can be briefly illustrated as follows. Since the metamaterial superlens is a linear

system, so all dynamical processes can be solved by sum of multi-frequency components. And each frequency component can be solved by sum of multi-wavevector components. So we can use Green's function of multi-frequency components to obtain the strict numerical results. Therefore, our method based on the Green's function is strict, and it is quite a universe method in any linear system, for example, it can be used to study the two dimensional (2D) and three dimensional (3D) metamaterial superlens.

The content of the chapter is organized as follows. We mainly focus on the details of our theory and method in Section 2. After that, in Section 3, we will calculate the field of the image of a NIR superlens by using our method, including radiative waves, evanescent waves, SEWs, and global field. The method will be confirmed by using FDTD simulations. In Section 4, we will present our study on the group delay of evanescent wave in the superlens by using our method. Finally, conclusions are presented in Section 5.

2. Theoretical method

In this section, we will focus on the theoretical details of our method. First, a time-dependent Green's function will be introduced. Then, based on the Green's function, the method to obtain evanescent waves as well as radiative waves will be presented.

2.1. A time-dependent Green's function

First, we would like to introduce a very useful time-dependent Green's function for the solution of inhomogeneous media. The time-dependent Green's function can be applied to study the dynamical scattering processes[7, 22]. In the inhomogeneous media, the problem we study can be solved by Maxwell equations:

$$\begin{aligned} \nabla \times \vec{E}(r,t) &= -\mu(r)\mu_0 \frac{\partial}{\partial t}\vec{H}(r,t), \\ \nabla \times \vec{H}(r,t) &= \epsilon(r)\epsilon_0 \frac{\partial}{\partial t}\vec{E}(r,t) + \vec{J}(r,t), \end{aligned} \tag{1}$$

where $\vec{J}(r,t) = \sigma(r,t)\vec{E}(r,t)$ is the current density and $\sigma(r,t)$ is the conductivity. We rewrite Eq.(1) as:

$$\nabla \times \nabla \times \vec{E}(r,t) + \epsilon(r)\mu(r)\epsilon_0\mu_0 \frac{\partial^2}{\partial t^2}\vec{E}(r,t) = -\mu(r)\mu_0 \frac{\partial}{\partial t}[\sigma(r,t)\vec{E}(r,t)] \tag{2}$$

To solve Eq.(2), we introduce a dynamic Green's function $\overrightarrow{\overrightarrow{G}}(r,r';t,t')$, which satisfies:

$$\left(\nabla \times \nabla \times + \epsilon(r)\mu(r)\epsilon_0\mu_0 \frac{\partial^2}{\partial t^2}\right) \overrightarrow{\overrightarrow{G}}(r,r';t,t') = \delta(r-r')\delta(t-t')\overrightarrow{\overrightarrow{I}} \tag{3}$$

where $\overrightarrow{\overrightarrow{I}}$ is a unit dyad. In this system, when r and r' is given, $\overrightarrow{\overrightarrow{G}}(r,r';t,t')$ is just a function of $(t-t')$ in time domain, so it yields

$$\overrightarrow{\overrightarrow{G}}(r,r';t,t') = \overrightarrow{\overrightarrow{G}}(r,r';t-t'). \tag{4}$$

Therefore, Eq.(3) becomes:

$$\left(\nabla \times \nabla \times +\epsilon(r)\mu(r)\epsilon_0\mu_0\frac{\partial^2}{\partial t^2}\right)\overrightarrow{\overrightarrow{G}}(r,r';t-t') = \delta(r-r')\delta(t-t')\overrightarrow{\overrightarrow{I}} \tag{5}$$

If $\overrightarrow{\overrightarrow{G}}(r,r';t-t')$ is known, then the $\vec{E}$ field can be found as

$$\vec{E}(r,t) = -\mu_0\int \overrightarrow{\overrightarrow{G}}(r,r';t-t')\cdot\vec{J}(r',t')dr'dt' \tag{6}$$

By Fourier transforming Eq.(5) from time domain to frequency domain, we obtain

$$\left(\nabla \times \nabla \times -\mu(r,\omega)\epsilon(r,\omega)\epsilon_0\mu_0\omega^2\right)\overrightarrow{\overrightarrow{G}}(r,r';\omega) = \delta(r-r')\overrightarrow{\overrightarrow{I}} \tag{7}$$

where $\epsilon(r,\omega)$ and $\mu(r,\omega)$ are the relative permittivity and the relative permeability of the dispersive material at a frequency ω, respectively, and $\overrightarrow{\overrightarrow{G}}(r,r';\omega)$ is the Green's Function in the frequency domain, which satisfies

$$\overrightarrow{\overrightarrow{G}}(r,r';t-t') = \frac{1}{2\pi}\int d\omega\overrightarrow{\overrightarrow{G}}(r,r';\omega)e^{-i\omega(t-t')} \tag{8}$$

By Fourier transforming the electric field $\vec{E}(r,t)$ in time domain to the frequency domain, we obtain $\vec{E}(r,\omega)$, satisfying

$$\vec{E}(r,t) = \frac{1}{2\pi}\int d\omega e^{-i\omega t}\vec{E}(r,\omega) \tag{9}$$

Considering the general properties:

$$\begin{aligned}\epsilon(r,-\omega) &= \epsilon(r,\omega)^*,\\ \mu(r,-\omega) &= \mu(r,\omega)^*,\end{aligned} \tag{10}$$

and

$$\overrightarrow{\overrightarrow{G}}(r,r';-\omega) = \overrightarrow{\overrightarrow{G}}(r,r';\omega)^*. \tag{11}$$

Substituting Eq.(8), Eq.(9), Eq(10) and Eq.(11) into Eq.(6), we can obtain

$$\vec{E}(r,\omega) = \overrightarrow{\overrightarrow{G}}(r,r';\omega)\cdot\vec{E}(r',\omega). \tag{12}$$

Eq.(12) exhibits the role of $\overrightarrow{\overrightarrow{G}}(r,r';\omega)$ that $\overrightarrow{\overrightarrow{G}}(r,r';\omega)$ is a propagator for the field in the frequency domain between r and r'. Here we have supposed that $\sigma(r',t) = 1$ in the source region for simplicity. If $\vec{E}(r',\omega)$ is the exciting source's electric field in the frequency domain, i.e., $\vec{E}_s(r',\omega) = \vec{E}(r',\omega)$, then Eq.(12) can be rewritten as:

$$\vec{E}(r,\omega) = \overrightarrow{\overrightarrow{G}}(r,r';\omega)\cdot\vec{E}_s(r',\omega) \tag{13}$$

where $\vec{E}_s(r',\omega)$ is the spectrum of the exciting source.

So the field $\vec{E}(r,t)$ can be obtained by the inverse Fourier transformation:

$$\vec{E}(r,t) = \frac{1}{2\pi}\int d\omega e^{-i\omega t}\vec{E}(r,\omega), \tag{14}$$

where ω_0 is the working frequency of the exciting source.

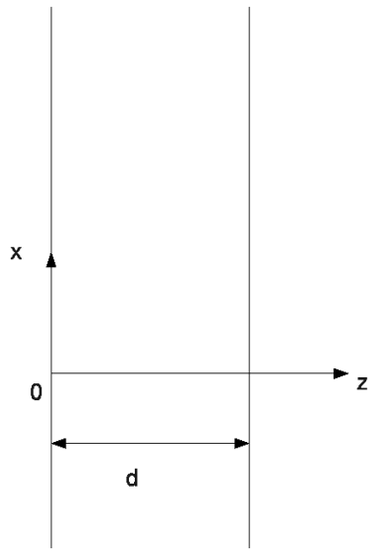

Figure 1. The shematic of the three-layer inhomogeneous medium.

Now the remaining problem is to solve Eq(7) to get $\overrightarrow{\overrightarrow{G}}(r,r';\omega)$. With the exciting source $E_s(r',t)$ (whose spectrum is $E_s(r',\omega)$), after obtain $\overrightarrow{\overrightarrow{G}}(r,r';\omega)$, then we can calculate $\vec{E}(r,\omega)$ directly by Eq.(12).

As a typical example, the time-dependent Green's function for the three-layer inhomogeneous media is presented, which is shown in Fig.1. The inhomogeneous media of the system can be described by:

$$\epsilon(r)\epsilon_0, \mu(r)\mu_0 = \begin{cases} \epsilon_0, \mu_0 & z > d \\ \epsilon_l^r\epsilon_0, \mu_l^r\mu_0 & 0 < z < d \\ \epsilon_0, \mu_0 & z < 0 \end{cases} \tag{15}$$

$\overrightarrow{\overrightarrow{G}}(r,r';\omega)$ is related to the transmission coefficient and/or reflection coefficient which are dependent on the boundary conditions of each layer. Here, we only consider the Green's function in the region that $z > d$. Under these conditions, $\overrightarrow{\overrightarrow{G}}(r,r';\omega)$ has been obtained in Ref.[7]. $\overrightarrow{\overrightarrow{G}}(r,r';\omega)$ is different in different spatial dimensions. For three-dimension, we can rewrite $\overrightarrow{\overrightarrow{G}}(r,r';\omega)$ as follows:

$$\begin{aligned} \overrightarrow{\overrightarrow{G}}(r,r';\omega) = &-\frac{i\sigma(r',\omega)}{8\pi}\int \frac{1}{k_z}e^{-ik_z z}[T^{TE}(k_\parallel)(J_0(k_\parallel x) - J_2(k_\parallel x)) \\ &+ \frac{k_z^2}{k^2}T^{TM}(k_\parallel)(J_0(k_\parallel x) + J_2(k_\parallel x))k_\parallel dk_\parallel], \end{aligned} \tag{16}$$

where $J_0(z)$ and $J_2(z)$ are the usual zeroth-order Bessel function and second-order Bessel function, respectively, and $k_{\|}^2 + k_{lz}^2 = \epsilon_l^r \mu_l^r (\omega/c)^2$, $k_{\|}^2 + k_z^2 = (\omega/c)^2$ are the dispersion relation in the region $(0 < z < d)$ and the region $(z < 0, z > d)$ respectively. Here, T^{TE} and T^{TM} are the transmission coefficients for TE wave ($\vec{H}$ polarized) and TM wave ($\vec{E}$ polarized), respectively, which are respectively given by

$$T^{TE}(k_{\|}) = \frac{4\triangle e^{-ik_z d}}{(\triangle+1)^2 e^{-ik_{lz}d} - (\triangle-1)^2 e^{ik_{lz}d}}, \tag{17}$$

and

$$T^{TM}(k_{\|}) = \frac{4\triangle' e^{-ik_z d}}{(\triangle'+1)^2 e^{-ik_{lz}d} - (\triangle'-1)^2 e^{ik_{lz}d}}, \tag{18}$$

where $\triangle = \dfrac{k_{lz}}{k_z \mu_l^r}$ and $\triangle' = \dfrac{k_{lz}}{k_z \epsilon_l^r}$.

$\sigma(r', \omega)$ is the conductivity in source region, i.e., $\vec{J}(r', \omega) = \sigma(r', \omega)\vec{E}_s(r', \omega)$. $\sigma(r', \omega)$ has been assumed to be $\sigma(r', \omega) = 1$. So Eq(16) becomes:

$$\begin{aligned} \overrightarrow{\overrightarrow{G}}(r, r'; \omega) = &- \frac{i}{8\pi} \int \frac{1}{k_z} e^{-ik_z z} [T^{TE}(k_{\|})(J_0(k_{\|}x) - J_2(k_{\|}x)) \\ &+ \frac{k_z^2}{k^2} T^{TM}(k_{\|})(J_0(k_{\|}x) + J_2(k_{\|}x)) k_{\|} dk_{\|}], \end{aligned} \tag{19}$$

For the 2D case, the wave vector $k_{\|} = k_x$, we have

$$\overrightarrow{\overrightarrow{G}}(r, r'; \omega) = -\frac{i}{4\pi} \int \frac{e^{ik_x x}}{k_z} T^{TE}(k_x) e^{ik_z z} dk_x. \tag{20}$$

And for the 3D case, we have

$$\overrightarrow{\overrightarrow{G}}(r, r'; \omega) = -\frac{i}{2k} T^{TE}(0) e^{-ikz}. \tag{21}$$

After $\overrightarrow{\overrightarrow{G}}(r, r'; \omega)$ is obtained, we can obtain the field in the frequency domain in the region $z > d$ by Eq.(12). And then by the inverse Fourier transformation, the field in time domain can be obtained.

2.2. The Green's function for radiative waves and evanescent waves

Now, we will apply a time-dependent Green's function for a radiative wave and an evanescent wave. This Green's function can be directly developed from the Green's function introduced in the Sec.2.1. The schematic model is shown in Fig.1. As we know, the plane solution wave for the electric field in vacuum is of the form $E_z(r_{||}, z, t) = E_{z0}\exp(i(k_{||}r_{||} + k_z z - \omega t))$, where $k_{||}$ and k_z are wave numbers along the xy plane and z directions respectively, and they satisfy the dispersion relation as follows: $k_{||}^2 + k_z^2 = \omega^2/c^2$, where c is the light velocity in the vacuum. In the case of $k_{||}^2 < \omega^2/c^2$, k_z is real, corresponding to the radiative waves along the z direction. While if $k_{||}^2 > \omega^2/c^2$, k_z is imaginary, corresponding to the evanescent waves along the z

direction. Similarly, in the slab region, the real or imaginary k_{lz} corresponds to the radiative wave or the evanescent wave along z direction, respectively.

For simplicity, we first consider the 2D system, in which $k_{||} = k_x$. The global field of image region is the superposition of radiative waves and evanescent waves. We can rewrite Eq.(20),Eq.(13) and Eq(14) as follows:

$$\overrightarrow{\overrightarrow{G}}(r,r';\omega;k_{min},k_{max}) = -\frac{i}{4\pi}\int_{k_{min}}^{k_{max}} \frac{e^{ik_x x}}{k_z} T^{TE}(k_x) e^{ik_z z} dk_x, \tag{22}$$

$$\vec{E}(r;\omega;k_{min},k_{max}) = \overrightarrow{\overrightarrow{G}}(r,r';\omega;k_{min},k_{max}) \cdot \vec{E}_s(r',\omega), \tag{23}$$

and

$$\vec{E}(r;t;k_{min},k_{max}) = \frac{1}{2\pi}\int d\omega e^{-i\omega t}\vec{E}(r;\omega;k_{min},k_{max}), \tag{24}$$

where $k_{min} < k_x < k_{max}$ is the integral range. The integral range is of great significance, since different integral range corresponds to different wave. For example, the integral range $[k_{min} \to -\infty, k_{max} \to \infty]$ is for global field, and the range $[k_{min} = -\omega/c, k_{max} = \omega/c]$ is for radiative wave. Obviously, for linear system, the integral range can be chosen arbitrarily.

From Eq.(22) to Eq.(24), we can directly calculate the radiative wave and evanescent wave. In the case of radiative wave ($k_x^2 < \omega^2/c^2$), the integral range is $[k_{min} = -\omega/c, k_{max} = \omega/c]$, so the radiative wave Green's function $\overrightarrow{\overrightarrow{G}}_{rad}(r,r';\omega)$ satisfies

$$\begin{aligned}\overrightarrow{\overrightarrow{G}}_{rad}(r,r';\omega) &= \overrightarrow{\overrightarrow{G}}(r,r';\omega;k_{min} = -\omega/c, k_{max} = \omega/c) \\ &= -\frac{i}{4\pi}\int_{-\omega/c}^{\omega/c} \frac{e^{ik_x x}}{k_z} T^{TE}(k_x) e^{ik_z z} dk_x\end{aligned} \tag{25}$$

for radiative waves.

In the case of evanescent wave ($k_x^2 > \omega^2/c^2$), the integral range is $k_x > |\omega/c|$, so the evanescent wave Green's function $\overrightarrow{\overrightarrow{G}}_{eva}(r,r';\omega)$ satisfies:

$$\begin{aligned}\overrightarrow{\overrightarrow{G}}_{eva}(r,r';\omega) &= 2\lim_{k_{max}\to\infty} \overrightarrow{\overrightarrow{G}}(r,r';\omega;k_{min} = \omega/c, k_{max}) \\ &= -\frac{i}{2\pi}\lim_{k_{max}\to\infty}\int_{\omega/c}^{k_{max}} \frac{e^{ik_x x}}{k_z} T^{TE}(k_x) e^{ik_z z} dk_x\end{aligned} \tag{26}$$

for evanescent waves.

And for the global field, the global field Green's function $\overrightarrow{\overrightarrow{G}}_{glob}(r,r';\omega)$ satisfies:

$$\overrightarrow{\overrightarrow{G}}_{glob}(r,r';\omega) = \overrightarrow{\overrightarrow{G}}_{rad}(r,r';\omega) + \overrightarrow{\overrightarrow{G}}_{eva}(r,r';\omega) \tag{27}$$

Additionally, we can also focus our observation on the *subdivided evanescent wave* (SEW), with a certain integral range $[k_{min} = k_x^a, k_{max} = k_x^b]$. The SEW, with a certain integral range, can

also be obtained from Eq.(22) to Eq.(24) such that

$$\begin{aligned}\overrightarrow{\overrightarrow{G}}_{SEW}(r,r';\omega)|_{k_{min}=k_x^a}^{k_{max}=k_x^b} &= \overrightarrow{\overrightarrow{G}}(r,r';k_x^a,k_x^b) \\ &= -\frac{i}{4\pi}\int_{k_x^a}^{k_x^b}\frac{e^{ik_x x}}{k_z}T^{TE}(k_x)e^{ik_z z}dk_x.\end{aligned} \tag{28}$$

As an typical example, a SEW with an integral range $[k_{min} = 1.1\omega/c, k_{max} = 1.2\omega/c]$, whose Green's function can be obtained easily from Eq.(28) as:

$$\overrightarrow{\overrightarrow{G}}_{SEW}(r,r';\omega)|_{k_{min}=1.1\omega/c}^{k_{max}=1.2\omega/c} = -\frac{i}{4\pi}\int_{1.1\omega/c}^{1.2\omega/c}\frac{e^{ik_x x}}{k_z}T^{TE}(k_x)e^{ik_z z}dk_x.$$

In this way, we can obtain the Green's function for the SEW with any integral range. Obviously, evanescent wave could be regarded as the superposition of SEWs. Therefore, we have

$$\overrightarrow{\overrightarrow{G}}_{eva}(r,r';\omega) = \sum_{SEWs}\overrightarrow{\overrightarrow{G}}_{SEW}(r,r';\omega). \tag{29}$$

From Eq.(28), Eq.(26), Eq.(25), and Eq.(27), one can obtain the SEW Green's function $\overrightarrow{\overrightarrow{G}}_{SEW}(r,r';\omega)$, the evanescent wave Green's function $\overrightarrow{\overrightarrow{G}}_{eva}(r,r';\omega)$, the radiative wave Green's function $\overrightarrow{\overrightarrow{G}}_{rad}(r,r';\omega)$, and the global field Green's function $\overrightarrow{\overrightarrow{G}}_{glob}(r,r';\omega)$, respectively. Substituting them to Eq.(23) and Eq.(24) respectively, we can obtain the field of the SEW, the evanescent wave, the radiative wave, and the global field, respectively.

For the 3D system, obviously, the methods to get Green's function for the SEW, the evanescent wave, the radiative wave, and the global field are respectively very similar with the above discussion, i.e., just replace k_x by $k_{||}$ and let $k_{||}^2 = k_x^2 + k_y^2$ in Eq.(28), Eq.(26), Eq.(25), and Eq.(27), respectively.

3. Electromagnetic waves in the image of the superlens

In this section, we will discuss the image's field of a 2D metamaterial superlens, which is shown in Fig.2. The thickness of the metamaterial slab is d, which is placed at the *xy-plane* between $z = d/2$ and $z = 3d/2$. The source is set in the object plane at ($z = 0$). Obviously, the image will be formed in the image plane at $z = 2d$. The source is the quasi-monochromatic random source with the field expressed as $E_s(r,t)$=$U_s(r,t)exp(-i\omega_0 t)$, where $U_s(r,t)$ is a slow-varying random function, $\omega_0 = 1.33 \times 10^{15}/s$ is the central frequency of our random source (the details of the random source can be seen in Ref.[29]). The exciting source $E_s(r,t)$ is a quasi-monochromatic field with the central frequency ω_0, whose electric field $\vec{E}_s(t)$ and frequency spectrum $\vec{E}_s(\omega)$ are shown in Fig.3(a) and Fig.3(b), respectively. In this paper, only the TM modes are investigated (the TM modes have the electric field perpendicular to the two-dimensional plane of our model).

The inhomogeneous media of the metamaterial superlens system are described by:

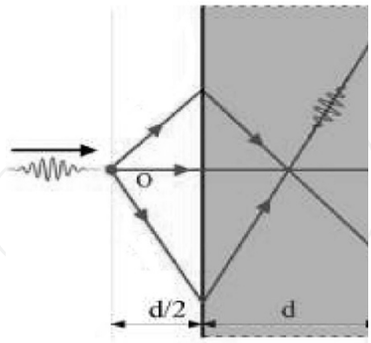

Figure 2. The schematic diagram of our model.

$$\epsilon(r),\mu(r) = \begin{cases} \epsilon_0,\mu_0 & z > 3/2d \\ \epsilon_0\epsilon_l^r,\mu_0\mu_l^r & 1/2d < z < 3/2d \\ \epsilon_0,\mu_0 & z < 1/2d \end{cases} \tag{30}$$

The negative relative permittivity ϵ_l^r and the negative relative permeability μ_l^r of metamaterial are phenomenologically introduced by the Lorenz model. The negative relative permittivity ϵ_l^r and the negative relative permeability μ_l^r are satisfied as follows:

$$\epsilon_l^r(\omega) = \mu_l^r(\omega) = 1 + \omega_p^2/(\omega_a^2 - \omega^2 - i\Delta\omega\cdot\omega) \tag{31}$$

where $\omega_a = 1.884 \times 10^{15}/s$ and $\Delta\omega = 1.88 \times 10^{14}/s$ are the resonant frequency and the resonant line-width of the "resonators" in the metamaterial respectively, and $\omega_p = 10 \times \omega_a$ is the plasma frequency. At $\omega = \omega_0$, we have $\epsilon_l^r = \mu_l^r = -1.0 + i0.0029$.

In order to excite the evanescent wave strong enough in the image of the metamaterial superlens, the distance $d/2$ between the source and the superlens should be small enough. Here we choose $d = \lambda_0/2$, where $\lambda_0 = 1.42\mu m$ is the wavelength corresponding to the central frequency ω_0.

For this metamaterial superlens system, it is very easy to obtain $\overrightarrow{\overrightarrow{G}}_{glob}(r,r';\omega)$, $\overrightarrow{\overrightarrow{G}}_{eva}(r,r';\omega)$, and $\overrightarrow{\overrightarrow{G}}_{SEW}(r,r';\omega)$ from Eq.(26) to Eq.(28), respectively. Let $r = 2d$ and $r' = 0$, and thus the Green's functions for the image will be obtained. After that, we can obtain the global field, the evanescent wave and the SEW of the image via:

$$\begin{aligned} \vec{E}_{glob}(2d,t) &= \frac{1}{2\pi}\int d\omega e^{-i\omega t}\vec{E}_{glob}(2d,\omega) \\ \vec{E}_{eva}(2d,t) &= \frac{1}{2\pi}\int d\omega e^{-i\omega t}\vec{E}_{eva}(2d,\omega) \\ \vec{E}_{SEW}(2d,t) &= \frac{1}{2\pi}\int d\omega e^{-i\omega t}\vec{E}_{SEW}(2d,\omega) \end{aligned} \tag{32}$$

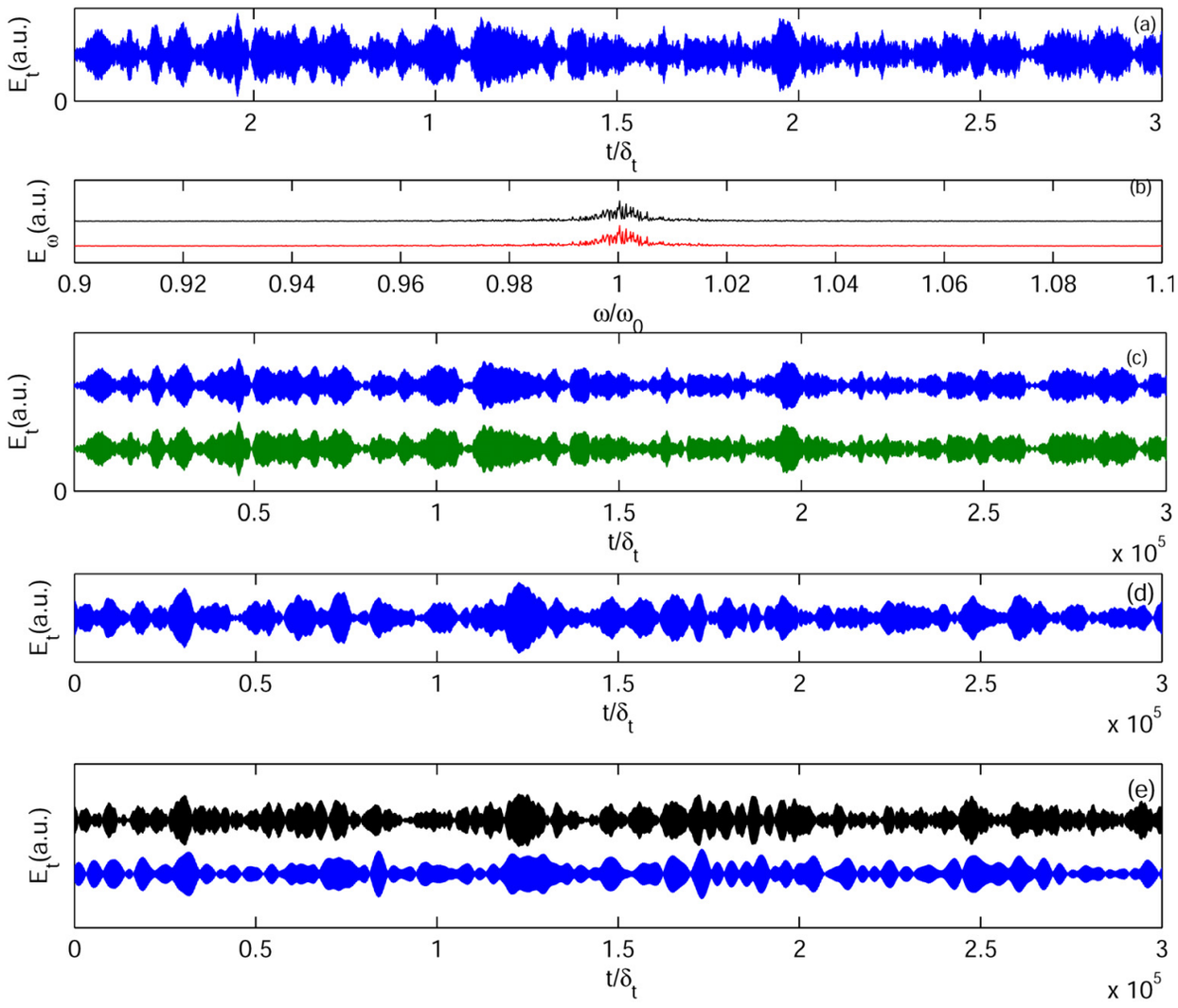

Figure 3. (a) Electric field of the source. (b) Spectrum of the source (top) and the image obtained by using our method (bottom) in units of ω_0. (c) Electric field of the image vs time. The global field calculated by using our method (top) and by using FDTD (bottom). (d) The evanescent wave of the image calculated by using our method. (e) Two typical SEWs of the image.

respectively, where

$$\begin{aligned}
\vec{E}_{glob}(2d,\omega) &= \overrightarrow{\overrightarrow{G}}_{glob}(2d,0;\omega)\cdot\vec{E}_s(\omega)\\
\vec{E}_{eva}(2d,\omega) &= \overrightarrow{\overrightarrow{G}}_{eva}(2d,0;\omega)\cdot\vec{E}_s(\omega)\\
\vec{E}_{SEW}(2d,\omega) &= \overrightarrow{\overrightarrow{G}}_{SEW}(2d,0;\omega)\cdot\vec{E}_s(\omega).
\end{aligned} \tag{33}$$

The numerical results calculated by our method are shown in Fig.3. Fig.3(c)(up, the blue one), (d) and (e) show the global field, the evanescent wave, and two typical SEWs respectively. The integral k_x range of the two SEWs are $[k_{min} = 1.1\omega/c, k_{max} = 1.2\omega/c]$ (shown in Fig.3(e)(up, the black one)), and $[k_{min} = 1.3\omega/c, k_{max} = 1.4\omega/c]$ (shown in Fig.3(e)(down, the blue one)), respectively.

In order to convince our method, FDTD simulation is also applied to calculate the field of the image, which is shown in Fig.3(c) (down, the green one). Comparison with the results calculated by our method and FDTD shown in Fig.3(c), we can see they coincide with each other very well. In addition, we also calculate the frequency sepctrum of the image by our method, as shown in Fig.3(b) (down, the red one). Comparing the spectra of source and image, we can find they are very close to each other. This result also agrees with the Ref.[29]. Therefore, our method is convincible, which can be used to obtain the pure evanescent waves, the SEWs, and the global field effectively.

4. Group delay time of SEWs and its impacts on the temporal coherence

4.1. Group delay time of SEWs

From Figs.3(c)-(e), we can find that the profile of evanescent wave and that of SEWs look like that of radiative wave with a group delay time τ_r. So the field evanescent wave $\vec{E}_{eva}(t)$, as well as that of SEWs $\vec{E}_{SEW}(t)$, can be written as an expression such as $\vec{E}_{eva(SEW)}(t) = f_a(t)\vec{E}_{rad}(t-\tau_r)$, where $f_a(\tau_r)$ is parameter function of τ_r. In order to quantitatively study the delay time τ_r, we introduce a function $y(\tau_i)$ which satisfies:

$$y(\tau_i) = \int_t dt |\vec{E}_{rad}(t)| \cdot |\vec{E}_{eva}(t-\tau_i)|, \tag{34}$$

where $\vec{E}_{rad}(t)$ and $\vec{E}_{eva}(t)$ are the field of radiative wave and the evanescent wave respectively, τ_i is an independent variable with the time dimension. Since the profile of the radiative wave and the evanescent wave are very similar, obviously, the function $y(\tau_i)$ will get the maximal value when $\tau_i = \tau_r$. Therefore, the delay time can be defined quantitatively as follows:

$$\tau_r = [Max(y(\tau_i))]^{-1}. \tag{35}$$

Here $[\cdots]^{-1}$ means the inverse function.

Similarly, we can also study the group delay time of the SEWs. We rewrite Eq.(34) as follows:

$$y(\tau_i) = \int_t dt |\vec{E}_{rad}(t)| \cdot |\vec{E}_{SEW}(t-\tau_i)|, \tag{36}$$

where $E_{SEW}(t)$ is the field of the SEW with a certain integral k_x range. So we can calculate the delay time of the SEWs from Eq.(36) and Eq.(35).

In our numerical experiment, in order to calculate the group delay time of the SEWs, we choose 70 SEWs with integral k_x range as $[k_{mx} - 0.01\omega_0/c,\ k_{mx} + 0.01\omega_0/c]$, where k_{mx}=$1.01\omega_0/c$, $1.02\omega_0/c$, $\cdots$, $1.69\omega_0/c$, $1.7\omega_0/c$, respectively. The delay time of the 70 SEWs is shown in Fig.4(a). In this figure, we can see that the SEW with larger integral variable k_x will have a larger delay time. Obviously, the function $\tau_r = \tau_r(k_x)$ is a continuous-monotone increasing function, when the integral range $[k_x - dk_x, k_x + dk_x]$ is infinitesimal ($dk_x \to 0$). The result can be obtained by using a polynomial fitting, as shown in Fig.4(a). Therefore, from Fig.4(a), we can find that the SEWs with larger integral variable k_x corresponds to a larger delay time, which means the group velocity of SEWs with larger integral variable is smaller in the superlens system.

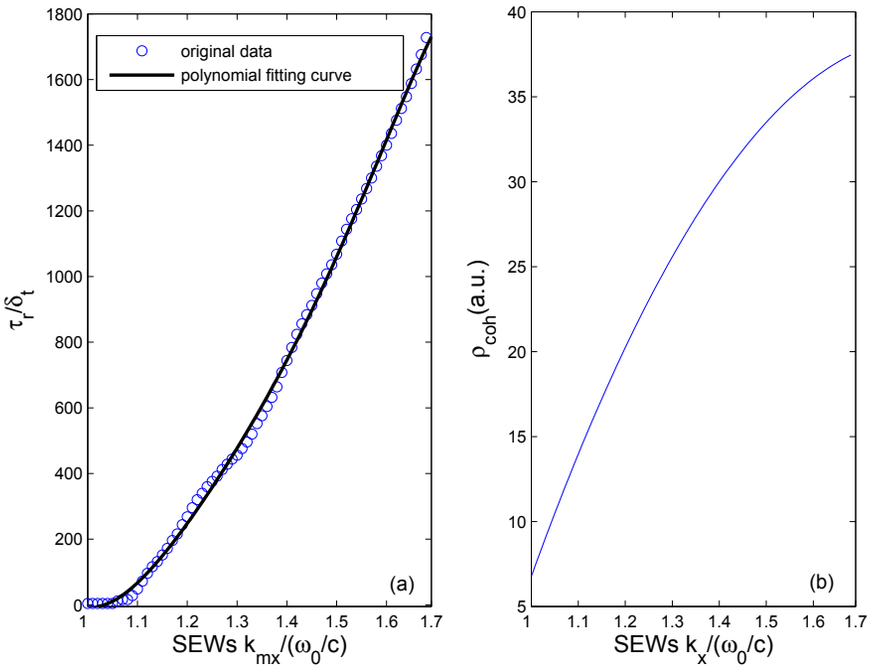

Figure 4. (a) The group delay time τ_r of SEWs. (b) ρ_{coh} of SEWs.

Since the field profile of SEWs looks like that of a radiative wave, so we can write the field of the SEW with the integral range $[k_x - \delta k_x, k_x + \delta k_x]$ as follows:

$$\vec{E}_{SEW}(t) = A(\tau_r(k_x))\vec{E}_{rad}(t - \tau_r(k_x)), \tag{37}$$

where $A(\tau_r(k_x)) = B(\tau_r(k_x))exp(-2|k_z(k_x)|d)$, $B(\tau_r)$ is a slowly-verifying function of τ_r, and $exp(-2|k_z|d)$ is an exponentially-decreasing function of k_z and a general-function of τ_r. Obviously, when τ_r(or k_x) becomes larger, $A(\tau_r)$ will trends to become smaller. Then the field of evanescent wave $\vec{E}_{eva}(t)$ can be obtained by:

$$\begin{aligned} \vec{E}_{eva}(t) &= \int \vec{E}_{SEW}(t)dk_x \\ &= \int A(\tau_r(k_x))\vec{E}_{rad}(t - \tau_r(k_x))dk_x. \end{aligned} \tag{38}$$

The physical meaning of $A(\tau_r)$ and its impacts will be discussed in the following.

4.2. Impacts of the group delay of SEWs on temporal coherence gain in the image of the superlens

One of the most interesting impacts of the group delay of SEWs is related to the first-order temporal coherence gain (CG). Here, we would like to discuss the CG caused by the SEWs in the image of the superlens. In our previous work [29, 30], we have investigated a prominent CG of the image by the radiative waves even when the frequency-filtering effects are very weak. Then, a natural question is what about the role of the evanescent waves play in the CG of a superlens? In this section, we will show that not only the radiative waves but also the evanescent waves, and the SEWs that can be responsible for the CG. Furthermore, we will show that the total CG in the image of a superlens is the weighted

averaged of evanescent-wave coherence gain (ECG), radiative-wave coherence gain (RCG), radiative-wave and evanescent-wave coherence gain (RECG).

First of all, let's consider the contributions of the evanescent waves on the CG. For this, we calculate the normalized first-order temporal coherence $g^{(1)}(r,\tau)$ of the superlens with the random source $E_s(t)$ exciting, which are shown in Fig.5. Here, the normalized first-order temporal coherence function $g^{(1)}(r,\tau)$ is defined by

$$g^{(1)}(r,\tau) = \frac{G^{(1)}(r,\tau)}{G^{(1)}(r,0)} = \frac{<\vec{E}^*(r,t)\vec{E}(r,t+\tau_r)>}{<\vec{E}^*(r,t)\vec{E}(r,t)>} \tag{39}$$

where $G^{(1)}(r,\tau)$ is a coherence function, which is defined by

$$G^{(1)}(r,\tau) =< \vec{E}^*(r,t)\vec{E}(r,t+\tau_r) > \tag{40}$$

or

$$G^{(1)}(r,\tau) = \lim_{T\to\infty}\frac{1}{2T}\int_{-T}^{T}\vec{E}^*(r,t)\vec{E}(r,t+\tau)dt, \tag{41}$$

here $< \cdots >$ means the statistic average (ensemble average) and τ is time delay. From Fig.5, we can see that the temporal coherence of image of evanescent wave, radiative wave and global field, are all obviously better than that of source. Comparing with the temporal coherence of source and image, there are three kinds of coherence gain as follows. The first one is the radiative-wave coherence gain (RCG, this mechanism has been discussed in our previous work[29, 30]), which is determined by the radiative waves. The second one is the evanescent-wave coherence gain (ECG), which is determined by the evanescent waves. The last one is the global field coherence gain (GCG), which is from the global field with the co-effect of RCG and ECG.

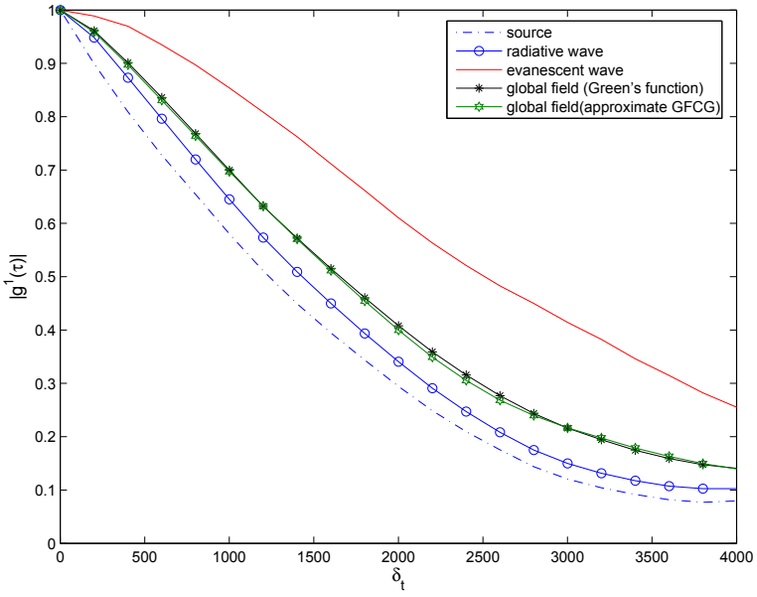

Figure 5. The first temporal coherence of image and source. The dashed-dotted one is the $g^{(1)}(r,\tau)$ of the source. Others are for the image, i.e., the red one, the black one (and also the green one), and the blue one are the $g^{(1)}(r,\tau)$ of the evanescent waves, the global field, and the radiative waves, respectively.

To show how the ECG is produced from the interference of the SEWs with different group delay time, we assume there are only two SEWs, such as $\vec{E}^{\alpha}_{SEW}(t)$ and $\vec{E}^{\beta}_{SEW}(t)$ with the range $[k^{\alpha}_{mx} - \delta k^{\alpha}_{mx}, k^{\alpha}_{mx} + \delta k^{\alpha}_{mx}]$ and $[k^{\beta}_{mx} - \delta k^{\beta}_{mx}, k^{\beta}_{mx} + \delta k^{\beta}_{mx}]$ respectively, which correspond to the delay time τ^{α}_r and τ^{β}_r, respectively. The two SEWs can be expressed by Eq.(37). We assume the two SEWs have an integral range very close to each other, i.e., $k^{\alpha}_{mx} \simeq k^{\beta}_{mx}$, and so we have $A(\tau_r(k^{\alpha}_{mx})) \simeq A(\tau_r(k^{\beta}_{mx}))$ and both of them are close to a certain constant A.

From Eq.(38), we have the evanescent wave field:

$$\begin{aligned} \vec{E}_{eva}(t) &= \vec{E}^{\alpha}_{SEW}(t) + \vec{E}^{\beta}_{SEW}(t) \\ &= A(\tau_r(k^{\alpha}_{mx}))\vec{E}_{rad}(t - \tau^{\alpha}_r) + A(\tau_r(k^{\beta}_{mx}))\vec{E}_{rad}(t - \tau^{\beta}_r) \\ &\simeq A \cdot (\vec{E}_{rad}(t - \tau^{\alpha}_r) + \vec{E}_{rad}(t - \tau^{\beta}_r)), \end{aligned} \tag{42}$$

then the temporal coherence of the evanescent wave in the image is given by

$$\begin{aligned} G_{eva}(\tau) =& < \vec{E}^{*}_{eva}(t)\vec{E}_{eva}(t + \tau) > \\ =& < \vec{E}^{*}_{rad}(t - \tau^{\alpha}_r)\vec{E}_{rad}(t - \tau^{\alpha}_r + \tau) + \vec{E}^{*}_{rad}(t - \tau^{\beta}_r)\vec{E}_{rad}(t - \tau^{\beta}_r + \tau) + \\ & \vec{E}^{*}_{rad}(t - \tau^{\alpha}_r)\vec{E}_{rad}(t - \tau^{\beta}_r + \tau) + \vec{E}^{*}_{rad}(t - \tau^{\beta}_r)\vec{E}_{rad}(t - \tau^{\alpha}_r + \tau) >, \end{aligned} \tag{43}$$

The first two terms are the same as the coherence function of the radiative wave, so they do not contribute to ECG. The last two terms are from the interference between SEWs, they can be very large at the condition $\tau \simeq |\tau^{\alpha}_r - \tau^{\beta}_r|$. This condition can always be satisfied between SEWs since τ_r is a continuous variable. So the relative delay time $|\tau^{\alpha}_r - \tau^{\beta}_r|$ of SEWs are responsible for ECG .

Therefore, ECG can always exist in the superlens when two conditions are satisfied: (1) $A(\tau_r(k^{\alpha}_{mx})) \simeq A(\tau_r(k^{\beta}_{mx}))$; and (2) $\tau \simeq |\tau^{\alpha}_r - \tau^{\beta}_r|$. Unfortunately, the two conditions could not always be satisfied at the same time. When $\tau \simeq |\tau^{\alpha}_r - \tau^{\beta}_r|$ is large, which also means the integral variable k^{α}_{mx} and k^{β}_{mx} are far from each other, so the value of $|A(\tau^{\alpha}_r) - A(\tau^{\beta}_r)|$ will be very large, and thus the former condition could not be satisfied. The condition that $A(\tau_r(k_x)) \simeq A(\tau_r(k_{mx}))$ is the direct reflection that ***only*** *the interference of those SEWs with* ***close*** *integral variable k_x can produce the ECG.*

Here the integral variable "k_x *close* to k_{mx}" means when k_{mx} is given, for any k_x satisfying $|k_x - k_{mx}| \rightarrow \delta k_{mx}$, the condition $A(\tau_r(k_x)) \simeq A(\tau_r(k_{mx}))$ is always satisfied, where δk_{mx} is a threshold value with small positive value near zero(for example δk_{mx}=0.01). For two SEWs with the integral range $[k_{mx} - \delta k_{mx}, k_{mx} + \delta k_{mx}]$ and $[k_x - \delta k_x, k_x + \delta k_x]$ respectively, we can obtain the relative delay time $\Delta\tau_r(k_x) = |\tau_r(k_x) - \tau_r(k_{mx})|$. As the discussion above, the relative delay time $\Delta\tau_r$ is responsible to the ECG. When k_x is *close* to k_{mx}, $\Delta\tau_r(k_x)$ is a monotonic increasing function of k_x in the range $[k_{mx}, k_{mx} + \delta k_{mx}]$, which gives a threshold value τ_d as:

$$\tau_d(k_x) = \lim_{k_x \rightarrow k_{mx} + \delta . k_{mx}} \Delta\tau_r(k_x) \tag{44}$$

τ_d shows the upper-limit of the effective coherent relative delay time that only the $\Delta\tau_r \leq \tau_d$ is the effective responsible to ECG. As $\Delta\tau_r$ increasing, when $\Delta\tau_r > \tau_d$, which means $|k_x - k_{mx}| > \delta k_{mx}$ (i.e. k_x and k_{mx} is not close to each other), the difference between $A(\tau_r(k_x))$ and $A(\tau_r(k_{mx}))$ becomes greater, and so their interference becomes weaker and their contribution to the coherence gain will decrease rapidly. While when $\Delta\tau_r \gg \tau_d$, which means the integral variable k_x and k_{mx} are very far from each other, then the SEW with the much larger integral variable one is too weak to have any effective interference, so their contribution to the coherence gain trends to be zero.

Therefore, the coherence gain from the interference of SEWs is limited by τ_d. The SEW with larger τ_d corresponds larger coherence gain. In order to study the temperas coherence gain of SEWs, we introduce a parameter function as: $\rho_{coh}(k_x) = \dfrac{d\tau_r(k_x)}{dk_x}$, which is shown in Fig.4(b). The physical meaning of $\rho_{coh}(k_x)$ is very clear, which gives a relation

$$\tau_d(k_x) \simeq \rho_{coh}(k_x) \cdot \delta k_x \tag{45}$$

when $\delta k_x \to 0$, we can get $\tau_d = \rho_{coh}\delta k_x$. Thus, τ_d is proportional to ρ_{coh}. From Fig.4(b) we can see that ρ_{coh} is an increasing function of k_x, so the SEWs with larger integral variable k_x correspond larger τ_d and stronger ECG, and so the field of the SEWs with larger integral various k_x will have better temporal-coherence $g^{(1)}(\tau)$.

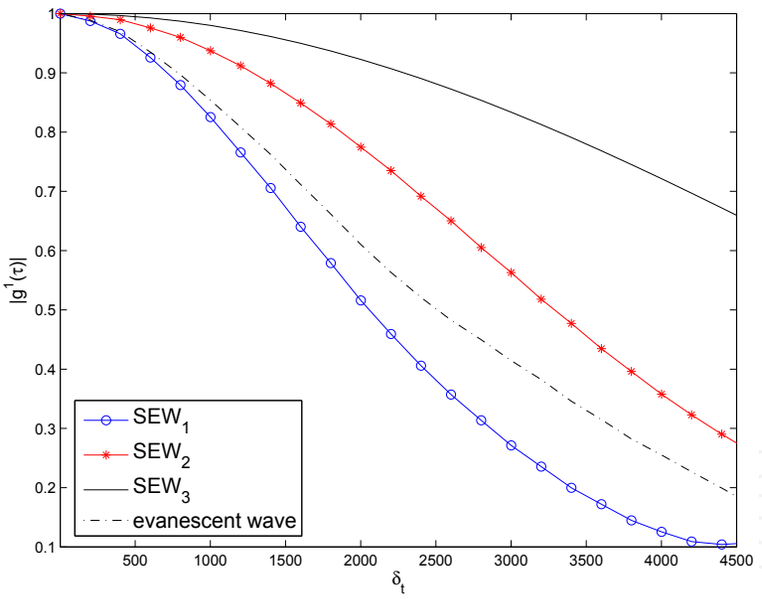

Figure 6. $g^{(1)}(\tau)$ of SEW_1, SEW_2, and SEW_3, comparing with $g^{(1)}(\tau)$ of evanescent wave.

To convince it, three SEWs (SWE_1,SWE_2,SWE_3)with the different integral k_x range $[k_{min} = 1.0\omega/c, k_{max} = 1.15\omega/c]$, $[k_{min} = 1.15\omega/c, k_{max} = 1.3\omega/c]$ and $[k_{min} = 1.3\omega/c, k_{max} = 1.45\omega/c]$ respectively are chosen to calculate the normalized first-order temporal-coherence function $g^{(1)}(\tau)$, which are shown in Fig.6. In this figure, we can see the temporal-coherence of SWE_3 with the largest integral variable is the best (black), the temporal coherence of SWE_2 with the second largest integral variable(red) is the second best, and the temporal coherence of SWE_1 with the smallest integral variable is the worst, which is expected.

5. Conclusion

In conclusion, based on the Green's function, we have numerically and theoretically obtained the evanescent wave, as well as the SEWs, separating from the global field. This study could help us to investigate the effect of an evanescent wave on a metamaterial superlens directly and give us a new way to design new devices.

Author details

Wei Li and Xunya Jiang
State Key Laboratory of Functional Materials for Informatics, Shanghai Institute of Microsystem and Information Technology, Chinese Academy of Sicences, Shanghai 200050, China

6. References

[1] V. C. Veselago, Sov. Phys. Usp. 10, 509 (1968).
[2] J. B. Pendry, Phys. Rev. Lett. 85, 3966 (2000).
[3] J. B. Pendry, Phys. Rev. Lett. 91, 099701 (2003).
[4] N. Garcia and M. Nieto-Vesperinas, Phys. Rev. Lett. 88, 207403 (2002).
[5] G. Gomez-Santos, Phys. Rev. Lett. 90, 077401 (2003).
[6] X. S. Rao and C. K. Ong, Phys. Rev. B 68, 113103 (2003).
[7] Y. Zhang, T. M. Grzegorczyk, and J. A. Kong, Prog. Electromagn. Res. 35, 271 (2002).
[8] L. Zhou and C. T. Chan, Appl. Phys. Lett. 86, 101104 (2005).
[9] Lei Zhou, Xueqin Huang and C.T. Chan, Photonics and Nanostructures 3, 100 (2005).
[10] Nader Engheta, IEEE Antennas and Wireless Propagation Lett. 1,10 (2002).
[11] Ilya V.Shadrivov, Andrey A.sukhorukov and Yuri S.Kivshar, Phys.Rev.E 67,057602 (2003).
[12] A.C.Peacock and N.G.R.Broderick,11,2502 (2003).
[13] R.A.Shelby,D.R.Smith,and S.Schultz, Science 292,77 (2001).
[14] E.Cubukcu,K.Aydin,E.Ozbay,S.Foteinopoulou,and C.M.Soukoulis,Nature 423,604 (2003)
[15] D. R. Smith, D. Schurig, M. Rosenbluth, S. Schultz, S.A.Ramakrishna, and J.B. Pendry, Appl. Phys. Lett. 82, 1506 (2003).
[16] X. S. Rao and C. K. Ong, Phys. Rev. E 68, 067601 (2003).
[17] S. A. Cummer, Appl. Phys. Lett. 82, 1503 (2003).
[18] P. F. Loschialpo, D. L. Smith, D. W. Forester, F. J. Rachford, and J. Schelleng, Phys. Rev. E 67, 025602(R) (2003).
[19] S.Foteinopoulou, E.N.Economou, and C.M.Soukoulis, Phys,Rev.Lett.90,107402 (2003).
[20] R. W. Ziolkowski and E. Heyman, Phys. Rev. E 64, 056625 (2001).
[21] L. Chen, S. L. He and L. F. Shen, Phys. Rev. Lett. 92, 107404 (2004).
[22] L. Zhou and C. T. Chan, Appl. Phys. Lett. 84, 1444 (2004).
[23] Michael W.Feise,Yuri S.Kivshar,Phys.Lett.A 334,326(2005).
[24] R. Merlin, Appl. Phys. Lett. 84, 1290 (2004).
[25] B.I.Wu, T.M.Grzegorczyk, Y.Zhang and J.A.Kong, J.Appl.Phys 93,9386 (2003).
[26] R.Ruppin, Phys.Lett.A 277,61(2000); R.Ruppin, J.Phys.:Condens.Matter 13,1811 (2001).
[27] W. Li, J. Chen, G. Nouet, L. Chen, and X. Jiang, Appl. Phys. Lett. 99, 051112 (2011).

[28] R. G. Hunsperger, Integrated Optics: Theory and Technology (Springer, New York, 1985).
[29] Peijun Yao, Wei Li, Songlin Feng and Xunya Jiang, Opt. Express 14, 12295 (2005).
[30] Xunya Jiang, Wenda Han, Peijun Yao and Wei Li, Appl. Phys. Lett. 89, 221102 (2006).